ELSEVIER

Journal of Organometallic Chemistry 498 (1995) 267–274

Journal of Organometallic Chemistry

Diastereomers of the carborane sandwich complex *commo*-[3,3-Fe{4-(Me_2S)-1,2-$C_2B_9H_{10}$}$_2$]; crystal structure of *meso*-[Fe($C_2B_9H_{10}SMe_2$)$_2$]

Yaw-Kai Yan, D. Michael P. Mingos *, David J. Williams

Department of Chemistry, Imperial College of Science, Technology and Medicine, South Kensington, London SW7 2AY, UK

Received 20 February 1995

Abstract

The crystal structure of *meso-commo*-[3,3'-Fe{4-(Me_2S)-1,2-$C_2B_9H_{10}$}$_2$], *meso*-**1**, has been determined. The molecules of the complex pack to form layers coincident with the [−1 0 1] planes. Both intra- and inter-molecular $BH^{\delta-} \cdots S^{\delta+}$ electrostatic interactions occur in the crystal, with H ··· S distances of 2.62 and 2.94 Å, respectively. These interactions can be regarded as involving reversed-polarity hydrogen bonds. The intermolecular interactions form a two-dimensional network within each of the molecular layers. The solid-state Raman spectrum of *meso*-**1** is clearly distinguishable from that of its DD/LL-isomers. The *p*-toluenesulfonate and bisulfate salts of the DD/LL-*commo*-[3,3'-Fe{4-(Me_2S)-1,2-$C_2B_9H_{10}$}$_2$]$^+$ cation have been synthesised in good yield by the oxidation of DD/LL-*commo*-[3,3'-Fe{4-(Me_2S)-1,2-$C_2B_9H_{10}$}$_2$] with *p*-benzoquinone.

Keywords: Boron; Iron; Carborane; Crystal structure

1. Introduction

Enantiomerism in borane and carborane cluster compounds can arise either from asymmetrical substitution of the cluster or from the introduction of chiral substituent groups. Asymmetrical substitution of the dicarbollide anion *nido*-[7,8-$C_2B_9H_{11}$]$^{2-}$, for example, affords chiral derivatives such as the D- and L-isomers of *nido*-[9-(Me_2S)-7,8-$C_2B_9H_{10}$]$^-$ and of *nido*-[7-phenyl-7,8-$C_2B_9H_{10}$]$^{2-}$ [1,2]. Bis(dicarbollyl)metal sandwich complexes synthesized from D/L racemates of chiral dicarbollide anions are in turn expected to exist as mixtures of DD, LL and DL (*meso*) diastereomers. The few reported studies on chiral boron cluster compounds [3] have generally indicated that it is difficult to fully resolve the enantiomers of chiral boron clusters, although some success has been achieved in the resolution of enantiomeric *B,B*- and *B,C*-disubstituted *nido*-[$C_2B_9H_{10}$RL] compounds (R = Me, Ph; L = Me_2S, pyridyl) by liquid chromatography [3f]. The diastereomers of the bis(dicarbollyl)metal complexes *commo*-[3,3'-M(1-R-1,2-$C_2B_9H_{10}$)$_2$]$^{n-}$ and *commo*-[3,3'-M(1-R-1,7-$C_2B_9H_{10}$)$_2$]$^{n-}$ [n = 2, 1, 0, for M = Fe(II), Co(III), Ni(IV), respectively; R = *m*- or *p*-fluorophenyl] were also reported to be inseparable [3c].

An investigation of the charge-transfer salts of metallacarborane complexes has led to the synthesis of the *meso*- and DD/LL-isomers of the bis(dicarbollyl)-iron(II) complex *commo*-[3,3'-Fe{4-(Me_2S)-1,2-$C_2B_9H_{10}$}$_2$] **1** (Fig. 1) [4]. A large difference in solubilities between the *meso*- and DD/LL-isomers of complex **1** was noted [4] and warranted further investigation. We reported the X-ray structure of the DD/LL-racemate of **1** previously [4]. An X-ray structural study was therefore carried out on *meso*-**1** both to confirm its structure and to see if any insight could be gained into the reasons underlying the low solubility of this isomer. Attempts were also made to synthesize salts of the DD/LL-*commo*-[3,3'-Fe{4-(Me_2S)-1,2-$C_2B_9H_{10}$}$_2$]$^+$ cations with chiral anions as a prelude for resolution studies. The syntheses and stabilities of the *p*-toluenesulfonate and bisulfate salts of DD/LL-*commo*-[3,3'-Fe{4-(Me_2S)-1,2-$C_2B_9H_{10}$}$_2$]$^+$ were also investigated, since there have been few detailed studies of cationic metallacarborane complexes [5].

---

* Corresponding author.

SSDI 0022-328X(95)05533-9

2. Results and discussion

2.1. Crystal structure of *meso*-[3,3'-Fe{4-(Me_2S)-1,2-$C_2B_9H_{10}$}$_2$], *meso*-1

The molecular structure of *meso*-**1** is shown in Fig. 2. The two icosahedral halves of the molecule are related by a crystallographically imposed inversion centre at (0, 0, 0), where the iron atom is located. This results in an *anti* disposition of the two Me_2S substituents and a staggered relationship for the dicarbollide cages. The C_2B_3 bonding faces are parallel and planar, with a maximum deviation of 0.009 Å from the mean plane [for B(7)]. The C–C and C–B bond lengths are normal (Table 3). The distance of the iron atom from each C_2B_3 plane is 1.50 Å, cf. 1.50 Å in the DD/LL-isomers [4]. The Fe–C distances [2.037(1)–2.039(1) Å] are significantly shorter than their Fe–B counterparts [2.103(2)–2.150(2) Å], resulting in a small shearing of the two C_2B_3 faces with respect to each other. These distances are very similar to the corresponding values observed in DD/LL–**1** [Fe–C 2.029(5)-2.057(4), Fe–B 2.084(5)–2.157(4) Å] [4]. The only other geometric feature of note is the directing of one of the hydrogen atoms [attached to B(7)/B(7a)] in each dicarbollide cage towards the sulfur atom attached to the other cage and vice versa. This hydrogen atom lies approximately *trans* to one of the methyl groups bonded to the sulfur [C(42)-S(41)-H(7a) 172°]. The B $\cdots$ S and H $\cdots$ S distances are 3.20 and 2.62 Å, respectively, and the B-H $\cdots$ S angle is 112°.

The molecules of *meso*-**1** pack to form layers coincident with the [-1 0 1] planes, as shown in Fig. 3. Within each layer, there is a two-dimensional network of weak intermolecular BH $\cdots$ S interactions (H $\cdots$ S 2.94 Å) involving the Me_2S groups in one molecule and the B(6)/B(6a)-bonded hydrogen atoms of another, with each hydrogen atom being approximately *trans* to the boron atom bonded to sulfur [B(4)–S(41)–H(6b) 165°]. Each molecule of *meso*-**1** is thus involved in four such interactions. These are somewhat weaker than the analogous intramolecular interactions. Both the intra-and inter-molecular BH $\cdots$ S interactions are probably mainly electrostatic in nature, with the formally monopositive sulfur atom acting as the acceptor for the hydridic boron-bonded hydrogen. The interactions can thus be considered as reverse-polarity hydrogen bonds. The hydridic nature of the boron-bonded hydrogen atoms of dicarbollide cages has been demonstrated in their ability to act as donor ligands in metal complexes [6]. The cooperative effect of the intermolecular "hydrogen-bonding" is probably an important contributary factor to the stability of the crystal lattice, and hence the low solubility, of *meso*-**1**. In contrast, in the structure of DD/LL-**1** there are no intermolecular distances shorter than van der Waals' contacts, indicating the absence of any significant directional intermolecular attractive forces in this crystal lattice [4].

The crystal packing of *meso*-**1** is also slightly more efficient than that of the DD/LL-isomers, as indicated by the calculated crystal densities (D_{calc}) and packing coefficients [7] (C_k) of these compounds (see Table 4). The more efficient packing of the *meso*-isomer is consistent with its being more discoidal in shape than the DD/LL-isomers [7a].

2.2. IR and Raman studies on the diastereomers of [3,3'-Fe{4-(Me_2S)-1,2-$C_2B_9H_{10}$}$_2$] 1

The X-ray crystallographic studies on DD/LL- and *meso*-**1** have shown that whilst the molecules of the former possess only molecular C_2 symmetry, molecules of the *meso*-isomer possess both molecular and crystallographic C_i symmetry. The solid-state IR and Raman spectra of *meso*-**1** are thus expected to contain fewer peaks than those of the DD/LL-isomers.

The important differences between the IR spectra of *meso*- and DD/LL-**1** are summarized in Table 5. It is

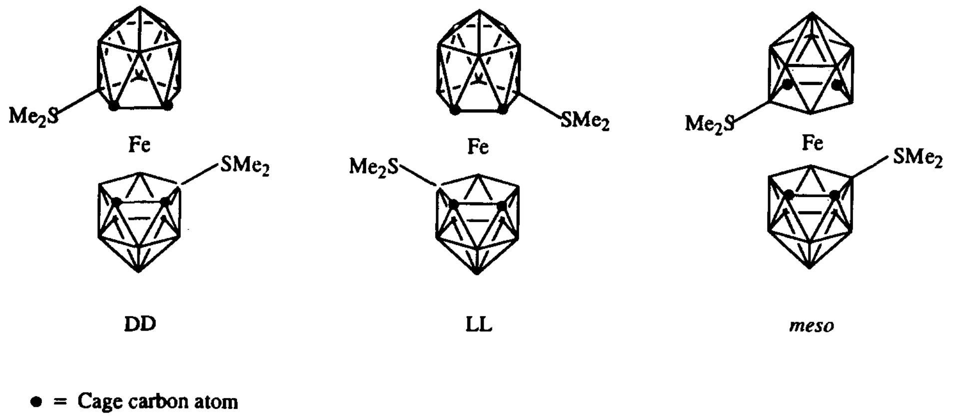

DD LL *meso*

● = Cage carbon atom

Fig. 1. Diagram of the diastereomers of complex 1.

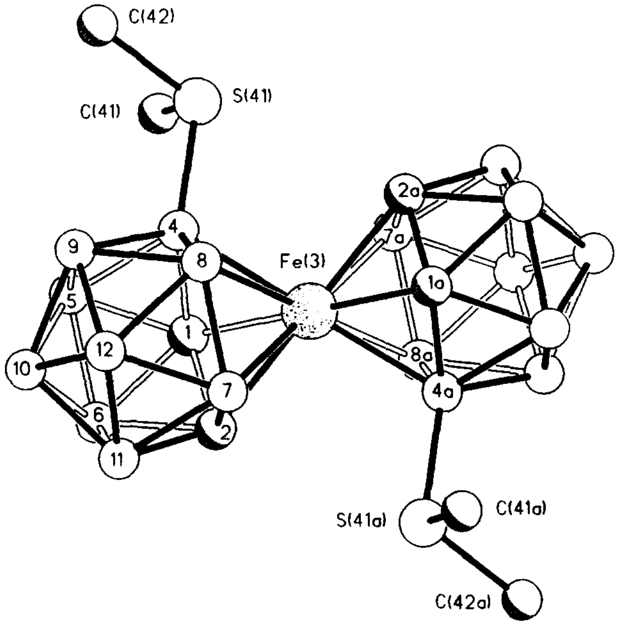

Fig. 2. Molecular structure of the *meso*-isomer of complex **1**, showing the atomic numbering scheme. The carbon atoms of the dicarbollide cages are hatched.

evident from Table 5 that there are fewer symmetry-allowed vibrational transitions for *meso*-**1**, in accordance with the presence of an inversion centre in the molecule.

The most useful part of the Raman spectrum of both *meso*-and DD/LL-**1** for diagnostic purposes is in the 3200–2400 cm^{-1} region. Two peaks assignable to the cage C–H stretching [ν(C–H, cage)] vibrations are present in the Raman spectrum of *meso*-**1**; they occur at 3032 and 3027 cm^{-1} respectively. However, the spec-

Table 1
Crystal and refinement data for *meso*-**1**

Crystal data	
Chemical formula	$C_8H_{32}B_{18}FeS_2$
M	442.9
Crystal system	monoclinic
Unit cell dimensions: a (Å)	12.274(3)
b (Å)	6.891(2)
c (Å)	13.501(4)
β (°)	105.49(2)
U (Å^3)	1100.4(5)
Space group	$P2_1/n$
D_c (g cm^{-3})	1.337
Z	2
F(000)	456
Color, habit	magenta needles
Crystal dimensions (mm)	0.27×0.33×0.53
μ (cm^{-1})	8.7 (Mo-Kα)
Data collection and processing	
Diffractometer	Siemens P4/PC
X-radiation λ (Å)	Mo-Kα (0.71073)
Scan mode	ω
scan width (°)	0.80
2θ limits (°)	3.0–60.0
No. of reflections:	
Total	3326
Unique R_{int} (%)	3201 (1.31)
Observed [$F > 4.0\sigma(F)$]	2792
Absorption correction	N/A
Structure analysis and refinement	
No. of parameters	165
Weighting scheme	$w^{-1} = \sigma^2(F) + 0.0007F^2$
R (observed data) (°)	2.73
R_w (observed data) (%)	3.18
Max., min. residual electron density (e A^{-3})	0.37, −0.30

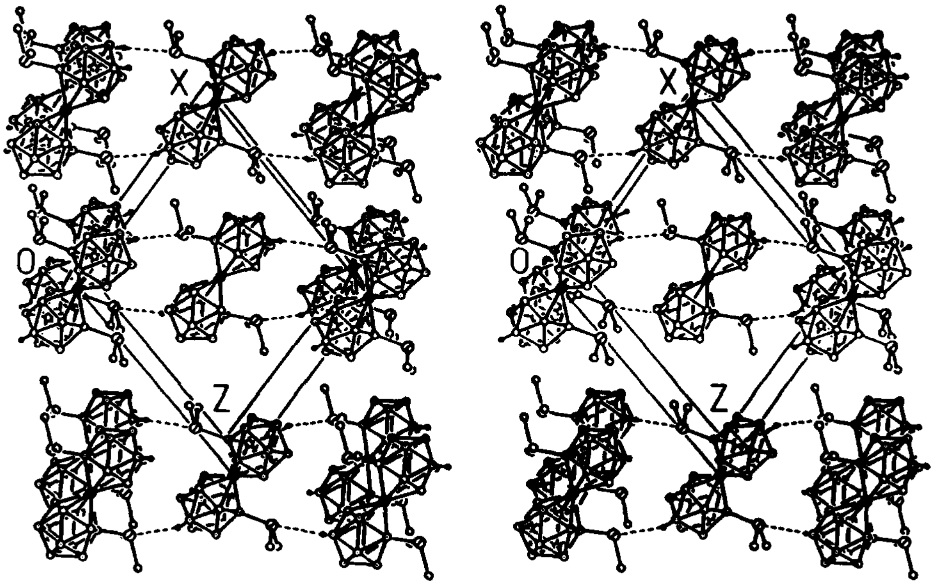

Fig. 3. Stereoscopic view of the molecular packing in *meso*-**1**, showing the BH · · · S interactions (indicated by dashed lines) within the layers of ferracarborane molecules.

Table 2
Atomic coordinates ($\times 10^4$) and equivalent isotropic displacement coefficients ($Å^2 \times 10^3$) for *meso*-1

	x	y	z	U_{eq} [a]
Fe(3)	0	0	0	20(1)
C(1)	−1381(1)	1489(2)	152(1)	24(1)
C(2)	−1599(1)	332(2)	−923(1)	26(1)
B(4)	−873(1)	−28(2)	1145(1)	25(1)
B(5)	−2319(1)	721(3)	829(1)	30(1)
B(6)	−2764(1)	986(2)	−512(1)	31(1)
B(7)	−1228(1)	−2045(2)	−727(1)	27(1)
B(8)	−763(1)	−2342(2)	626(1)	28(1)
B(9)	−1960(1)	−1752(3)	1113(1)	32(1)
B(10)	−3136(1)	−1115(3)	63(1)	32(1)
B(11)	−2678(1)	−1296(3)	−1072(1)	31(1)
B(12)	−2189(1)	−2998(2)	−68(1)	32(1)
S(41)	6(1)	903(1)	2464(1)	30(1)
C(41)	−499(1)	3317(2)	2589(1)	37(1)
C(42)	−542(2)	−342(3)	3405(1)	50(1)

[a] Equivalent isotropic U defined as one third of the trace of the orthogonalized U_{ij} tensor.

Table 3
Selected bond lengths (Å) and angles (°) for *meso*-1

Fe(3)–C(1)	2.039(1)	C(2)–B(7)	1.702(2)
Fe(3)–C(2)	2.037(1)	B(4)–B(8)	1.761(2)
Fe(3)–B(4)	2.103(2)	B(7)–B(8)	1.774(2)
Fe(3)–B(7)	2.104(2)	B(4)–S(41)	1.929(2)
Fe(3)–B(8)	2.150(2)	S(41)–C(41)	1.799(2)
C(1)–C(2)	1.615(2)	S(41)–C(42)	1.805(2)
C(1)–B(4)	1.683(2)		
C(1)–C(2)–B(7)	111.2(1)	C(2)–C(1)–B(4)	110.3(1)
C(2)–B(7)–B(8)	105.7(1)	B(4)–S(41)–C(41)	105.8(1)
B(4)–B(8)–B(7)	105.5(1)	B(4)–S(41)–C(42)	105.7(1)
C(1)–B(4)–B(8)	107.3(1)	C(41)–S(41)–C(42)	99.8(1)

Table 4
Some parameters [a] of DD/LL- and *meso*-1 which are associated with their molecular shapes and packing

	DD/LL-**1**	*meso*-**1**
D_{calc} (g cm^{-3})	1.323	1.337
C_k (%)	67.6	68.6
F_s	0.41	0.25
F_c	0.54	0.61
F_d	0.46	0.68

[a] $C_k = Z(V_{mol}/V_{cell}) \times 100$; Z = number of molecules in the unit cell; V_{mol} = molecular volume, calculated using the method of Ref. [7]; V_{cell} = volume of the unit cell; F_s = spherical index = M_3/M_1; F_c = cylindrical index = $1-[(M_2+M_3)/2M_1]$; F_d = discoidal index = $1-[2M_3/(M_1+M_2)]$; M_1, M_2 and M_3 are the moments of inertia of the molecule ($M_1 \geqslant M_2 \geqslant M_3$), which are calculated without mass weighting [7]. The closer the values of these indices are to unity, the closer the molecule is to the geometry represented by the index [7a].

Table 5
The main differences between the IR spectra of *meso*- and DD/LL-**1** [a]

	meso-**1**	DD/LL-**1**
ν(C–H, cage)	3031w, 3012w	3029w, 3019w, 3002w (sh)
ν(C–H, methyl)	2927w	2929w (sh), 2923w
ν(B–H) envelope		
$\tilde{\nu}_{max}$ (FWHM)	2548vs (140)	2527vs (180)
Peaks at 1144, 1119, 1066, 962, 778 and 722	absent or very weak	medium to strong

[a] All values in cm^{-1}.

trum of DD/LL-**1** shows four peaks for the ν(C–H, cage) vibrations, which occur at 3031, 3025, 3017 and 3006 cm^{-1}, respectively. The observed number of Raman-active ν(C–H, cage) normal modes for both *meso*-**1** (point group C_i) and DD/LL-**1** (point group C_2) agree with the predictions of group theory [8]. The spectrum of DD/LL-**1** exhibits three peaks due to the methyl C–H stretching vibrations (2935, 2930 and 2925 cm^{-1}), whilst that of the *meso*-isomer shows only one peak at 2931 cm^{-1}. The B–H stretching [ν(B–H)] peaks of DD/LL-**1** also span a wider range of wavenumbers than those of *meso*-**1**.

It is noteworthy that the number of ν(B–H) peaks in the Raman spectra of both *meso*- and DD/LL-**1** exceed the theoretical numbers of five and ten, respectively, based on the crystallographic symmetry of the molecules. In addition, although the ν(B–H) IR absorptions of DD/LL-**1** are not well resolved, the IR spectrum of *meso*-**1** shows at least nine distinct ν(B–H) absorptions instead of five. This phenomenon has been observed in other boron cage compounds, and has been attributed to correlation splitting due to the presence of more than one molecule of the compound in the unit cell [9]. The magnitude of the isotopic (^{11}B and ^{10}B) splitting of the ν(B–H) bands of $[B_{12}H_{12}]^{2-}$ has been calculated to be $\leqslant 1$ cm^{-1} [9] and hence this effect is not likely to contribute significantly in complex **1**.

2.3. Synthesis and characterisation of [DD/LL-$Fe(C_2B_9H_{10}SMe_2)_2]^+[A]^-$ (2, A = p-$MeC_6H_4SO_3$; 3, A = HSO_4)

One of the aims of this study was to resolve the DD/LL-isomers of **1** via fractional recrystallization of the mixed salts [DD/LL-$Fe(C_2B_9H_{10}SMe_2)_2]^+[\chi]^-$, where $[\chi]^-$ is a chiral anion. Owing to the absence of strongly oxidizing precursors for chiral anions, it is not possible to synthesize salts of the DD/LL-$[Fe(C_2B_9H_{10}SMe_2)_2]^+$ cations with chiral anions via direct charge-transfer reactions. An alternative general synthetic route is thus required for DD/LL-$[Fe(C_2B_9H_{10}SMe_2)_2]^+$ salts. As a preliminary study, the preparation of salts of the DD/LL-$[Fe(C_2B_9H_{10}SMe_2)_2]^+$ cations with the nonchiral anions $[p\text{-}MeC_6H_4SO_3]^-$ and $[HSO_4]^-$ was investigated, and the results are presented below.

2.3.1. Synthesis

The compound DD/LL-**1** reacted with *p*-benzoquinone and *p*-toluenesulfonic acid in dichloromethane–acetone (8 : 3) solution to form a fine reddish-brown precipitate of $[\text{DD/LL-Fe}(C_2B_9H_{10}SMe_2)_2]^+[p\text{-}MeC_6H_4SO_3]^-$ **2** in 94% yield:

$2\,[FeL_2] + 2\,MeC_6H_4SO_3H \qquad 2\,[FeL_2]^+[MeC_6H_4SO_3]^-$

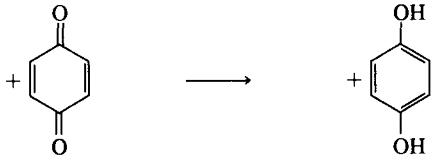

$(L = C_2B_9H_{10}SMe_2)$

The product was analytically pure even prior to recrystallization.

When the reaction was repeated with sulfuric acid in place of *p*-toluenesulfonic acid and dichloromethane instead of dichloromethane–acetone mixture, a brick-red precipitate of crude $[\text{DD/LL-Fe}(C_2B_9H_{10}SMe_2)_2]^+[HSO_4]^-$ **3** was obtained (87% crude yield). Pure blood-red crystals of compound **3** were obtained by recrystallization from acetonitrile (67% overall yield). The salt $[\text{DD/LL-Fe}(C_2B_9H_{10}SMe_2)_2]^+[HSO_4]^-$ is very soluble in methanol, ethanol, dimethylsulfoxide (DMSO) and acetone, moderately soluble in acetonitrile and insoluble in water. In contrast, $[\text{DD/LL-Fe}(C_2B_9H_{10}SMe_2)_2]^+[p\text{-}MeC_6H_4SO_3]^-$ **2** is insoluble or sparingly soluble in most of the common solvents except DMSO, in which it dissolves readily. Dilute solutions of compounds **2** and **3** are light orange in color, whilst concentrated solutions are deep reddish-brown.

Both compounds **2** and **3** are air- and moisture-stable solids. Solutions of the compounds are very sensitive, however, towards reduction by aqueous, methanolic or ethanolic basic media. Aqueous and alcoholic solutions of both the carbonate and bicarbonate ions are sufficiently basic to cause reduction. The redox reactions involved are probably the following:

$$2\,[FeL_2]^+ + 2\,[OH]^- \longrightarrow 2\,[FeL_2] + H_2O_2$$

$$2\,[FeL_2]^+ + 2\,[RCH_2O]^-$$

$$\longrightarrow 2\,[FeL_2] + RCHO + RCH_2OH$$

$$L = C_2B_9H_{10}SMe_2;\ R = H,\ Me$$

Compound **3** is also rapidly reduced by boiling methanol or ethanol, although the reaction does not occur at an appreciable rate at room temperature:

$$2\,[FeL_2]^+ + RCH_2OH \rightarrow 2\,[FeL_2] + RCHO + 2\,H^+$$

The oxidation process based on *p*-benzoquinone, which had worked successfully for the syntheses of compounds **2** and **3**, could not be used for the preparation of their *meso*-analogs because of the poor solubility of *meso*-$[Fe(C_2B_9H_{10}SMe_2)_2]$ in acetone and dichloromethane.

2.3.2. Spectroscopic characterisation

The IR spectra of compounds **2** and **3** (as KBr pellets) exhibit an intense, broad absorption band at ca. 2560 cm^{-1}, which is assigned to the B–H stretching vibrations of the $\text{DD/LL-}[Fe(C_2B_9H_{10}SMe_2)_2]^+$ cations. This represents a high-energy shift of ca. 35 cm^{-1} for the B–H stretching absorptions when $\text{DD/LL-}[Fe(C_2B_9H_{10}SMe_2)_2]$ is oxidized to its cationic form. The C–H stretching absorptions of the dicarbollide cages (3017 cm^{-1}) and the SMe_2 groups (2970 and 2940 cm^{-1}) of the $\text{DD/LL-}[Fe(C_2B_9H_{10}SMe_2)_2]^+$ cations in **3** are all considerably more intense than the corresponding absorptions in $\text{DD/LL-}[Fe(C_2B_9H_{10}SMe_2)_2]$. For compound **2**, the peaks in the 3020–2930 cm^{-1} region cannot be unambiguously assigned to the $[Fe(C_2B_9H_{10}SMe_2)_2]^+$ cations since the $[p\text{-}MeC_6H_4SO_3]^-$ anion also absorbs in this region. The spectra of compounds **2** and **3** are dominated by strong absorption peaks of their anions between 1300 and 500 cm^{-1}, where the spectra closely resemble those of $p\text{-}MeC_6H_4SO_3H.H_2O$ and $KHSO_4$, respectively [10].

The UV–vis absorption bands of compound **3** in acetonitrile are summarized in Table 6. All the absorptions are assigned to the $\text{DD/LL-}[Fe(C_2B_9H_{10}SMe_2)_2]^+$ cations since the $[HSO_4]^-$ anion ($[NEt_4]^+$ salt, 2.6 mmol dm^{-3} CH_3CN solution) does not absorb in the 200–900 nm spectral region. There are no previous reports of the UV-vis spectra of cationic bis (dicarbollyl) metal complexes.

2.4. Attempted synthesis of $[DD/LL\text{-}Fe(C_2B_9H_{10}SMe_2)_2]^+[\chi]^-$ [χ = (1S)-10-camphorsulfonate, S-2-methylbutanoate]

The choice of chiral anions for the resolution of $\text{DD/LL-}[Fe(C_2B_9H_{10}SMe_2)_2]^+$ is limited by the highly oxidising nature of the complex. The commonly employed tartrate anion, for example, is unsuitable because it contains secondary alcohol functional groups (see Fig. 4), which are susceptible towards oxidation to ketones.

Table 6
UV–visible absorptions of compound **3** [a]

λ_{max} (nm)	ε ($dm^3\ mol^{-1}\ cm^{-1}$)
242 (sh)	13000
276	17300
300 (sh)	16600
424 (sh)	760
488 (sh)	520
544 (sh)	340
578 (sh)	320

[a] Measured in CH_3CN (0.033 and 0.33 mmol dm^{-3} solutions used).

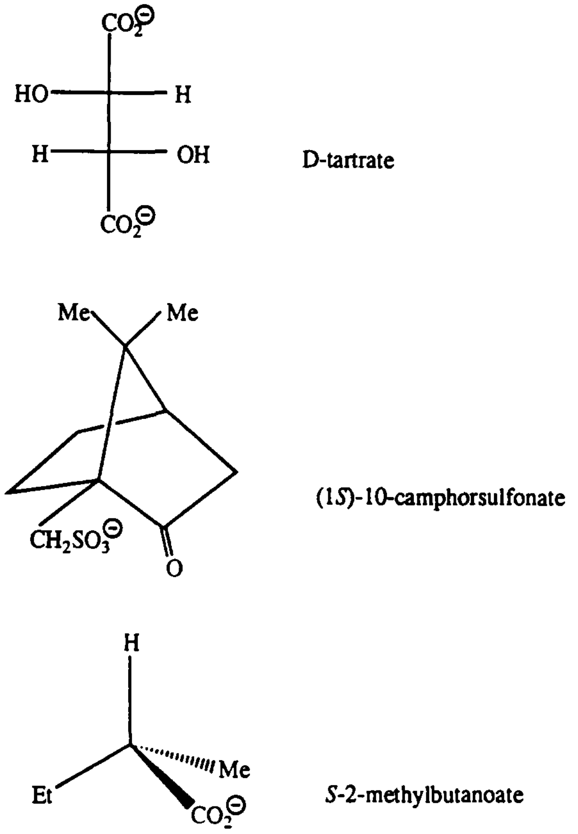

Fig. 4. Molecular structures of D-tartrate, (1*S*)-10-camphorsulfonate and *S*-2-methylbutanoate anions.

The nonreducing chiral anions (1*S*)-10-camphorsulfonate ($[camSO_3]^-$) and *S*-2-methylbutanoate (Fig. 4) were chosen for this study because their conjugate acids are commercially available.

On addition of (1*S*)-10-camphorsulfonic acid to an orange–pink solution of DD/LL-$[Fe(C_2B_9H_{10}SMe_2)_2]$ and *p*-benzoquinone in dichloromethane, the solution turned orange–brown. No precipitation occurred, however, even when the solution was kept at −20°C for 90 min. Thin-layer chromatography (tlc) of the solution revealed that most of the starting materials remained unreacted. Comparison of this result with those obtained with *p*-toluenesulfonic acid and sulfuric acid suggests that the main driving force for the formation of compounds **2** and **3** is the precipitation of these salts from the reaction solution. Attempts were thus made to precipitate [DD/LL-$Fe(C_2B_9H_{10}SMe_2)_2]^+[camSO_3]^-$ from the reaction mixture by layering the solution with hexane, diethyl ether or toluene. Whilst layering with hexane resulted in the formation of colorless needles of $[camSO_3H]$ and some brown oil, crystals of $[camSO_3H]$ provided the only precipitate when toluene was used as the layering component. No precipitation occurred when diethyl ether was used.

No reaction occurred between DD/LL-$[Fe(C_2B_9H_{10}SMe_2)_2]$, *p*-benzoquinone and *S*-2-methylbutanoic acid in dichloromethane, as shown by tlc. This can be attributed to the lower acid dissociation constant of the carboxylic acid compared with those of the sulfonic acids and sulfuric acid.

3. Conclusions

Although difficulties have been encountered previously in the synthesis and purification of cationic bis(dicarbollyl)metal complexes [5a,b], this study has shown that the complex DD/LL-$[Fe(C_2B_9H_{10}SMe_2)_2]^+$ is stable and can be synthesised in good yield as the *p*-toluenesulfonate and bisulfate salts. Presumably the synthetic route developed above, based on oxidation by *p*-benzoquinone, produces the cationic complex in a form which may be isolated more easily. The precipitation of the salts from the reaction solution is probably an important driving force for their formation. The molecules of *meso*-$[Fe(C_2B_9H_{10}SMe_2)_2]$ possess both molecular and crystallographic inversion symmetry in the solid state. This contrasts with the crystal structure previously reported for DD/LL-$[Fe(C_2B_9H_{10}SMe_2)_2]$ [4], where no crystallographic symmetry is imposed on the molecules. The solid-state Raman spectrum of *meso*-$[Fe(C_2B_9H_{10}SMe_2)_2]$ is thus clearly distinguishable from that of the DD/LL-isomers. (The ^1H NMR and UV–vis spectra of the isomers are also clearly distinguishable) [4]. There are, however, no significant differences between the bonding within the molecules of *meso*- and DD/LL-**1**. The B–H stretching peaks of both *meso*- and DD/LL-**1** are better resolved in the Raman spectra of these complexes than in their IR spectra. The very low solubility of *meso*-**1**, which leads to its unusually facile separation from DD/LL-**1**, may be attributed to the existence of two-dimensional networks of intermolecular electrostatic $BH^{\delta-} \cdots S^{\delta+}$ interactions in the crystal. The cooperative effect of these interactions would be expected to increase the stability of the crystal lattice.

4. Experimental details

4.1. General

The commercially available compounds *p*-toluenesulfonic acid monohydrate (BDH), (1*S*)-10-camphorsulfonic acid (Aldrich), *S*-2-methylbutanoic acid (Aldrich) and $[NEt_4][HSO_4]$ (Fluka) were used as received; *p*-benzoquinone (BDH) was vacuum-sublimed before use. The compounds DD/LL- and *meso*-$[Fe(C_2B_9H_{10}SMe_2)_2]$ were made as previously described [4]. Reagent grade organic solvents were used.

4.2. Physical measurements

IR spectra were recorded on either a Perkin Elmer 1725X FT–IR spectrometer (for DD/LL- and *meso*-**1**) or a Perkin Elmer 1720 Fourier-transform spectrometer (for compounds **2** and **3**). Raman spectra were recorded on a Perkin Elmer NIR FT–Raman 1700X spectrometer equipped with a NdYAG laser (1064 nm); microcrystalline samples were loaded in glass melting-point capillaries. UV–vis spectra were obtained using a Perkin Elmer Lambda 2 UV/VIS spectrophotometer.

4.3. Syntheses

4.3.1. [DD / LL-Fe($C_2B_9H_{10}SMe_2$)$_2$]$^+$[p-MeC_6H_4-SO_3]$^-$ 2

A solution of *p*-$MeC_6H_4SO_3H \cdot H_2O$ (25 mg, 0.13 mmol) in acetone (15 cm^3) was added at room temperature to a stirred solution of DD/LL-[Fe($C_2B_9H_{10}$-SMe_2)$_2$] (26 mg, 0.059 mmol) and *p*-benzoquinone (8 mg, 0.07 mmol) in dichloromethane (40 cm^3). The resultant reddish-brown mixture was stirred at room temperature for 1 h, during which a fine reddish-brown precipitate of [DD/LL-Fe($C_2B_9H_{10}SMe_2$)$_2$]$^+$[*p*-$MeC_6H_4SO_3$]$^-$ **2** was formed. The precipitate was isolated by suction-filtration through a glass fiber filter, washed with acetone and dried under vacuum for 1 h. Yield: 34 mg, 94% (Found: C, 29.2; H, 6.1 $C_{15}H_{39}B_{18}FeO_3S_3$ requires C, 29.3; H, 6.4%); $\tilde{\nu}_{max}$ cm^{-1}) 3020s(sh), 2990s, 2929m (methyl CH), 2580vs(sh) (BH), 2566vs (BH), 2552vs (BH), 1426m, 1210vs (S=O), 1188vs (S=O), 1122s, 1107m, 1033s, 1010vs, 977m, 925w, 819m, 682vs, 563s (δ_{O-S-O}) (KBr).

4.3.2. [DD / LL-Fe($C_2B_9H_{10}SMe_2$)$_2$]$^+$[HSO_4]$^-$ 3

A 2.2% (w/v) solution of H_2SO_4 in acetonitrile (1.3 cm^3, equivalent to 29 mg H_2SO_4, 0.30 mmol) was added to a stirred solution of DD/LL-[Fe($C_2B_9H_{10}$-SMe_2)$_2$] (95 mg, 0.21 mmol) and *p*-benzoquinone (26 mg, 0.24 mmol) in dichloromethane (70 cm^3). A fine brick-red precipitate separated immediately. The mixture was stirred at room temperature for 50 min and then cooled to ca. −20°C. The cold mixture was filtered using a filter cannula and the residue was dried under vacuum. Crude yield: 99 mg, 87%. A 84 mg amount of the crude product was dissolved in acetonitrile (ca. 100 cm^3) at 30°C. The solution was filtered and slowly evaporated under reduced pressure in a warm water bath (ca. 50°C) to a volume of ca. 2 cm^3; a substantial amount of microcrystals were formed during evaporation. The mixture was left overnight at −35°C and then filtered while cold to obtain 65 mg (77% recovery) of compound **3** (Found: C, 17.7; H, 6.1%. $C_8H_{33}B_{18}FeO_4S_3$ requires C, 17.8; H, 6.2%); $\tilde{\nu}_{max}$ (cm^{-1}) 3017s (cage CH), 2970s(sh) and 2940s (methyl CH), 2558vs, br (BH), 1427s, 1331m, 1311w, 1222vs (S=O), 1185vs (S=O), 1081m, 1042vs, 1007s, 976s, 924m, 857m, 831s, 734m, 585s, br (δ_{O-S-O}) (KBr).

4.4. X-ray crystallography

Single crystals of *meso*-[Fe($C_2B_9H_{10}SMe_2$)$_2$] were grown by slow evaporation of an acetone solution of the compound at room temperature. The crystal data and refinement parameters for the compound are summarised in Table 1, fractional atomic coordinates are given in Table 2 and selected bond lengths and angles in Table 3.

The structure was solved by direct methods. Positional and anisotropic thermal parameters for nonhydrogen atoms were refined by the full-matrix least-squares method. Hydrogen atoms of the Me_2S group were introduced in calculated positions and refined isotropically. Those on the carborane cage were located by difference-Fourier syntheses and refined with the bond length constraints C–H 0.960 ± 0.002 and B–H 1.080 ± 0.002 Å and assigned isotropic thermal parameters $U(H) = 1.2\ U_{eq}(C, B)$. Calculations were performed on a VAX station 3100 model 76 computer using the SHELXTL PLUS software package [11].

Complete lists of bond lengths and angles and tables of hydrogen atom coordinates and anisotropic displacement parameters have been deposited at the Cambridge Crystallographic Data Centre.

References

[1] J. Plešek, Z. Janoušek and S. Heřmánek, *Collect. Czech. Chem. Commun., 43* (1978) 2862.

[2] M.F. Hawthorne, D.C. Young, T.D. Andrews, D.V. Howe, R.L. Pilling, A.D. Pitts, M. Reintjes, L.F. Warren, Jr. and P.A. Wegner, *J. Am. Chem. Soc., 90* (1968) 879.

[3] (a) M.F. Hawthorne, D.C. Young, P.M. Garrett, D.A. Owen, S.G. Schwerin, F.N. Tebbe and P.A. Wegner, *J. Am. Chem. Soc., 90* (1968) 862; (b) L.F. Warren, jr. and M.F. Hawthorne, *J. Am. Chem. Soc., 92* (1970) 1157; (c) R.G. Adler and M.F. Hawthorne, *J. Am. Chem. Soc., 92* (1970) 6174; (d) J.L. Little, P.S. Welcker, N.J. Loy and L.J. Todd, *Inorg. Chem., 9* (1970) 63; (e) J. Plešek, S. Heřmànek and B. Stíbr, *Pure Appl. Chem., 63* (1991) 399; (f) J. Plešek, B. Grüner and P. Maloň, *J. Chromatogr., 626* (1992) 197.

[4] Y.-K. Yan, D.M.P. Mingos, T.E. Müller, D.J. Williams and M. Kurmoo, *J. Chem. Soc., Dalton Trans.,* (1994) 1735.

[5] (a) M.F. Hawthorne, L.F. Warren, jr. K.P. Callahan and N.F. Travers, *J. Am. Chem. Soc., 93* (1971) 2407; (b) H.C. Kang, S.S. Lee, C.B. Knobler and M.F. Hawthorne, *Inorg. Chem., 30* (1991) 2024; (c) C.J. Jones, J.N. Francis and M.F. Hawthorne, *J. Am. Chem. Soc., 95* (1973) 7633; (d) N.L. Douek and A.J. Welch, *J. Chem. Soc., Dalton Trans.,* (1993) 1917.

[6] (a) J.A. Long, T.B. Marder, P.E. Behnken and M.F. Hawthorne, *J. Am. Chem. Soc., 106* (1984) 2979; (b) C.B. Knobler, T.B. Marder, E.A. Mizusawa, R.G. Teller, J.A. Long, P.E. Behnken and M.F. Hawthorne, *J. Am. Chem. Soc., 106* (1984) 2990;

(c) J.A. Long, T.B. Marder and M.F. Hawthorne, *J. Am. Chem. Soc., 106* (1984) 3004; (d) P.E. Behnken, J.A. Belmont, D.C. Busby, M.S. Delaney, R.E. King, III, C.W. Kreimendahl, T.B. Marder, J.J. Wilczynski and M.F. Hawthorne, *J. Am. Chem. Soc., 106* (1984) 3011; (e) J.A. Doi, R.G. Teller and M.F. Hawthorne, *J. Chem. Soc., Chem. Commun.,* (1980) 80; (f) I.T. Chizhevsky, I.A. Lobanova, V.I. Bregadze, P.V. Petrovskii, V.A. Antonovich, A.V. Polyakov, A.I. Yanovskii and Y.T. Struchkov, *Mendeleev Commun.,* (1991) 47; (g) Y.-W. Park, J. Kim and Y. Do, *Inorg. Chem. 33,* (1994) 1.

[7] (a) D.M.P. Mingos and A.L. Rohl, *J. Chem. Soc., Dalton Trans.,* (1991) 3419; (b) A.L. Rohl, VOLUME, *a program for the calculation of molecular volumes and moments of inertia,* University of Oxford, 1991.

[8] F.A. Cotton, *Chemical Applications of Group Theory,* Wiley–Interscience, New York, 3rd edn., 1990, Chap. 10, pp. 304–347.

[9] L.A. Leites, *Chem. Rev., 92* (1992) 279.

[10] C.J. Pouchert, *The Aldrich Library of FT–IR Spectra,* Aldrich Chemical Co., Inc., Milwaukee, Wisconsin, Edition 1, 1985, Vol. 2.

[11] G.M. Sheldrick, SHELXTL PLUS, Version 4.2, Siemens Analytical X-Ray Instruments Inc., Madison, WI, 1990.